# Experimental Study of Interfacial Fracture Toughness in a SiN$_x$/PMMA Barrier Film

Yongjin Kim,[†,‡] Anuradha Bulusu,[†,‡] Anthony J. Giordano,[†,§] Seth R. Marder,[†,§] Reinhold Dauskardt,[∥] and Samuel Graham*,[†,‡,⊥]

[†]Center for Organic Photonics and Electronics (COPE), [‡]Woodruff School of Mechanical Engineering, [⊥]School of Materials Science and Engineering, and [§]School of Chemistry and Biochemistry, Georgia Institute of Technology, Atlanta, Georgia 30332, United States

[∥]School of Materials Science and Engineering, Stanford University, Stanford, California 94305, United States

**ABSTRACT:** Organic/inorganic multilayer barrier films play an important role in the semihermetic packaging of organic electronic devices. With the rise in use of flexible organic electronics, there exists the potential for mechanical failure due to the loss of adhesion/cohesion when exposed to harsh environmental operating conditions. Although barrier performance has been the predominant metric for evaluating these encapsulation films, interfacial adhesion between the organic/inorganic barrier films and factors that influence their mechanical strength and reliability has received little attention. In this work, we present the interfacial fracture toughness of a model organic/inorganic multilayer barrier (SiN$_x$−PMMA). Data from four point bending (FPB) tests showed that adhesive failure occurred between the SiN$_x$ and PMMA, and that the adhesion increased from 4.8 to 10 J/m$^2$ by using a variety of chemical treatments to vary the surface energy at the interface. Moreover, the adhesion strength increased to 28 J/m$^2$ by creating strong covalent bonds at the interface. Overall, three factors were found to have the greatest impact on the interfacial fracture toughness which were (a) increasing the polar component of the surface energy, (b) creating strong covalent bonds at the organic/inorganic interface, and (c) by increasing the plastic zone size at the crack tip by increasing the thickness of the PMMA layer.

**KEYWORDS:** multilayer barrier, flexible organic electronics, mechanical failure, interfacial fracture toughness, chemical treatment, surface energy, polar component, plastic zone size
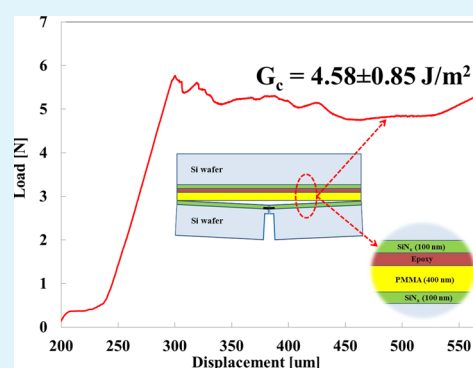
## 1. INTRODUCTION

The development of high-performance barrier films is seen as a critical technology for the packaging of organic electronic devices. Barriers consisting of inorganic films[1−4] or inorganic/organic multilayers[5−9] have been developed to provide effective water vapor transmission rates below $1 \times 10^{-5}$ g/m$^2$/day in order to improve the lifetime of devices, which are typically sensitive to water vapor and oxygen. For flexible applications or applications subjected to mechanical loading, concerns over the mechanical integrity of the barrier films have been studied primarily by analyzing the strain to failure or the critical bending radius that induces cracking of the inorganic layer[10−14] as such damage provides direct pathways for environmental species to permeate through the electronic package and degrade the device. In an effort to understand the mechanical performance of thin inorganic barriers, Leterrier et al. performed comprehensive experiments defining the crack onset strain (COS) of thin inorganic films with various film thicknesses (SiN$_x$: 80−800 nm and SiO$_x$: 30−160 nm) using a fragmentation test, and found that random cracks are initiated from microdefects that inherently exist in the inorganic films.[10−12] In addition, Leterrier et al. also experimentally investigated the interfacial strength between inorganic films and

organic substrates using the saturation damage approach found from uniaxial tensile loading.[15] Lewis et al. also investigated mechanical failure modes for inorganic films in the form of cracking and debonding using a collapsing radius test, and reported the crack density for 100 nm SiO$_x$N$_x$ film versus bending strain.[13,14] Although the strain to failure is important, the potential loss of adhesion of the laminate is also critical. Moreover, the adhesion at these interfaces can change over time especially when the barrier is subjected to outdoor environments leading to failure.[16,17] Whereas most of the research has focused on strain to failure in inorganic barriers on plastic substrates, very little research has focused on the fundamentals of adhesion in multilayer hybrid barriers.

It is well-known that interfacial adhesion between an inorganic and an organic film is composed of mechanical bonding, secondary bonding through weak van der Waals forces between molecules at the interface, and primary bonding through the formation of strong covalent bonds. Although mechanical adhesion is formed because of interlocking from
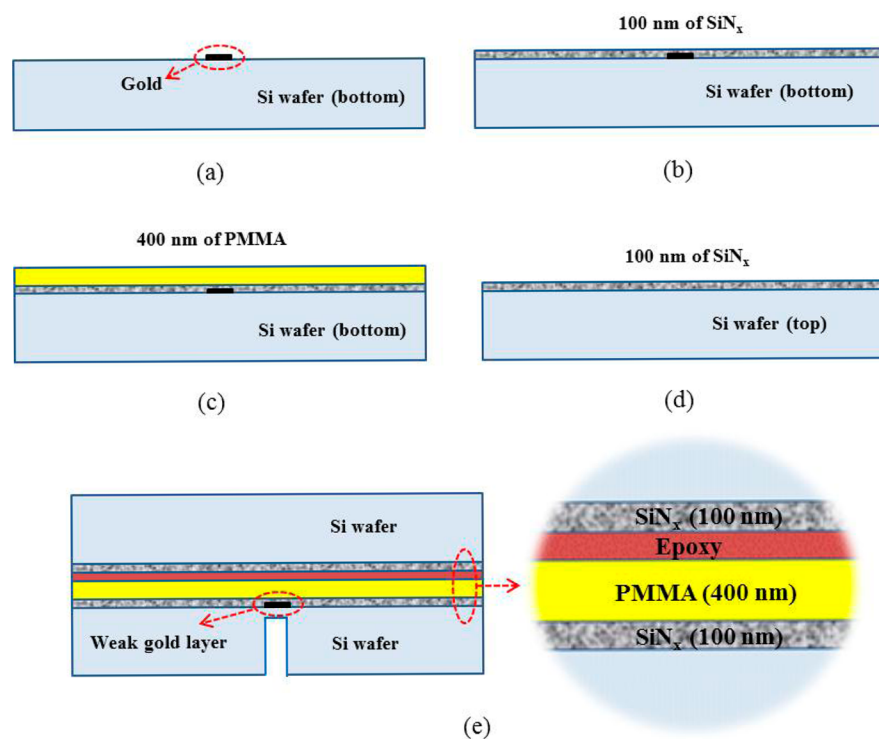
**Figure 1.** Schematic diagram of a typical sample structure: (a) deposition of Au strip (20 nm), (b) deposition of SiN$_x$ (100 nm), (c) spin-cast PMMA (400 nm), (d) deposition of SiN$_x$ (100 nm) on another Si wafer, and (e) a cross-sectional image of final sample bonded by a room-temperature curing epoxy (EPO-TEK 301).

surface roughness and filling in voids/defects on the surface, the secondary bonding, or van der Waals interactions, can be enhanced by having a chemical affinity between the materials in direct contact.[18,19] In general, van der Waals forces can be divided into three components, i.e., Keesom force (force between two permanent dipoles), Debye force (force between a permanent dipole and a corresponding induced dipole), and London dispersion force (force between two instantaneously induced dipoles).[20] The permanent dipole interactions (Keesom and Debye forces) can be assessed by measuring the polar component of the surface energy, whereas the instantaneously induced dipole interactions (London dispersion force) can be obtained from the dispersive component of the surface energy. By correlating the polar and dispersive components of the surface energy with interfacial fracture toughness, it will be possible to better understand how van der Waals forces play a role in the mechanical integrity of the interface.

To address the dearth of information on the adhesion of inorganic/organic barrier films, we performed a series of four point bending (FPB) tests to measure interfacial fracture toughness data using silicon nitride/polymethyl methacrylate interfaces (SiN$_x$–PMMA) as a model barrier film. Methods of improving the adhesion between the organic and inorganic barrier layers were investigated through surface treatments as well as through mechanical modification of the structure. Surface treatments to improve interfacial adhesion between SiN$_x$ and PMMA consisted of three different methods. The first method involved the use of oxygen plasma treatment as well as the addition of polar capping layers to improve the polarity of the interface. The second method consisted of phosphonic acids (PAs) as chemical modifiers that help enhance the secondary bonding at the interface through van der Waals

forces. Phosphonic acids consist of a headgroup that covalently binds to the substrate, a spacer group consisting of an alkyl chain, and a tail group whose polarity can be modified through the appropriate choice of functional groups.[21] The PA tail groups were tailored (a) to have a chemical affinity to PMMA by matching their chemical structure with that of PMMA, and (b) to vary the surface energy at the interface so as to increase the secondary bond strength between and SiN$_x$ and PMMA. The surface energies of individual substrates were quantified by contact-angle measurements to determine the polar and dispersive components of the surface energy. As a final step, surface energies, calculated by measured contact angles, were correlated and/or compared with measured interfacial fracture toughness data to determine the parameters that govern the interfacial adhesion between two contact surfaces. The third treatment to enhance interfacial adhesion was explored through the formation of primary bonds between SiN$_x$ and PMMA by using an organosilane-based surface modification technique. This method was previously reported by Prucker et al.[22] and used to modify the surface of silicon nitride by creating strong covalent bonds.[23−26] Benzophenone derivatives of organosilanes have also long been used to improve the adhesion strength of polymer based interfaces but to the best of our knowledge, there is very limited quantitative adhesion data reported thus far.[27−30] Dauskardt et al. used FPB tests for an organosilane ($\gamma$−methacyloxypropyltrimethoxy with acrylic monomers) treated Co−Cr−Mo prosthetic surface coated with PMMA film and found the interfacial adhesion strength to improve by a factor of 2.[23] However, silane modification techniques have never been adopted to maximize the adhesion strength of barrier structures and therefore, in this study, the interfacial adhesion strength using benzophenone derivatives of organosilanes was explored and compared with the other
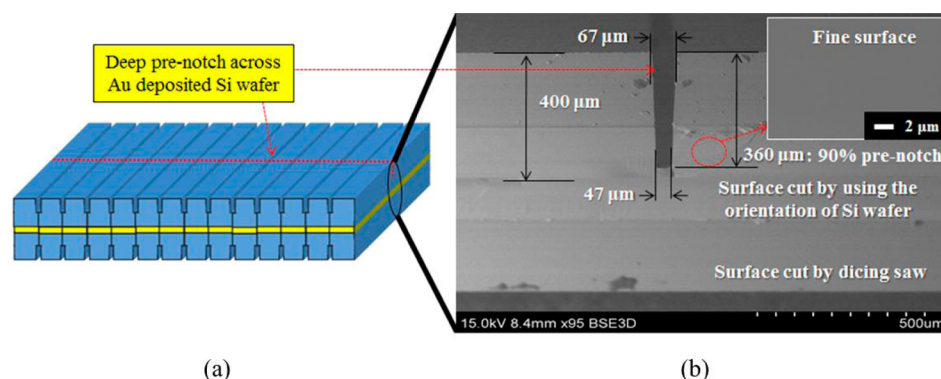
**Figure 2.** (a) Bonded Si wafer with prenotch using a dicing saw and (b) cross sectional SEM image of four point bending (FPB) sample surfaces cut by a dicing saw with an inset showing fine surface which was created by using the orientation of Si wafer.

methods described above. This study involved the formation of two different covalent bonds at the $SiN_x$–PMMA interface. The first covalent bond was formed between $SiN_x$ and the headgroup of the organosilane through silanization reactions[24] and the second covalent bond was formed between the benzophenone tail group and PMMA through photochemical reactions initiated by illumination with UV light.[22,29] In addition to the three surface treatment approaches, mechanical modification of the barrier structure to vary the plastic zone size at the crack tip and its impact on interface adhesion was explored through the variation of the PMMA layer thickness. Overall, we expect that this study of interfacial adhesion enhancement will provide valuable insight into the various methods that can be used to increase the interfacial fracture toughness in hybrid organic/inorganic barrier layers.

## 2. SAMPLE FABRICATION AND TESTING METHODS

**2.1. Sample Fabrication.** Samples for the interfacial fracture experiments were made by depositing bilayers of $SiN_x$ and PMMA onto standard Si wafers. First, a thin strip of gold (thickness, 20 nm; width, 8 mm) was deposited on a silicon (Si) wafer using e-beam deposition, as shown in Figure 1a. The gold (Au) layer plays a critical role as the crack path controller during the four point bending tests used to characterize the interfacial fracture toughness, and will be explained in detail later in section 2.2. Following the deposition of the gold strip, 100 nm of silicon nitride ($SiN_x$) was deposited over the Au deposited Si wafer using plasma enhanced chemical vapor deposition (PECVD) at 110 °C, as shown in Figure 1b. Next, PMMA (polymethyl methacrylate: $[CH_2C(CH_3)$-$(CO_2CH_3)]_n$, Av. M. W. = 120 000, Spectrum Chemicals & Laboratory Products, item: P2845) was prepared by mixing with toluene in a weight ratio of 1:15, and baked on a hot plate at 80 °C for 12 h. The PMMA solution was then spin-cast on the $SiN_x$ layer previously deposited on top of the gold layer followed by annealing at 110 °C for 30 min to remove any residual solvent in the PMMA film, as shown in Figure 1c. Another 100 nm of $SiN_x$ layer was also deposited on top of a separate Si wafer (Figure 1d) and bonded to the Au–$SiN_x$–PMMA coated Si wafer using a room temperature curing epoxy (EPO-TEK 301) cured at room temperature for 2 days. Post curing, the bonded wafers were cut into 45 mm × 5 mm pieces using a high speed dicing saw with a very thin blade (30 $\mu$m). A cross-sectional image of one such sample image is shown in Figure 1e.

To increase the yield of the FPB test, it was necessary to reduce possible damage near the notch root due to the low damage tolerance of the Si wafer. Thus, to reduce the defects, a dicing saw was used to make prenotches, down to 60% of the depth of the Si wafer, on the top and bottom of the Si wafer, as shown in Figure 2a. After creating the prenotches on top and bottom of the bonded wafer, a sharp diamond scriber was used to break the wafers into the final 45 mm × 5 mm FPB samples along the orientation of the Si wafer. As shown in Figure 2b with an inset image, the fracture of the Si along crystallographic planes resulted in very smooth and low damage surfaces for the subsequent deep prenotch used to initiate the fracture in four point bend (FPB) test. As a final step, a single deep prenotch across the bonded Si layer, was made on the top substrate down to 80–90% through the thickness of the Au deposited Si wafer (Figure 2). This deep prenotch serves an important role as the crack initiation point. Without this prenotch, it becomes impossible to control the crack initiation, leading to sample failure at random locations during the bending tests. Thus, by initiating the vertical crack at the deep prenotch during the FPB tests, the crack reaches the gold layer that eventually changes the direction of the crack propagation from vertical to horizontal ensuring its travel along the desired interface.

**2.2. Four Point Bending (FPB) Tests.** The interfacial fracture toughness is considered to be the macroscopic work of fracture per unit area ($G_c$, J/m$^2$) required to separate an interface.[17] This work of separation is determined by two different energy dissipating processes, the near-tip work of fracture ($G_o$) and energy dissipation ($G_{zone}$) due to inelastic deformation in the crack tip.[31] In this study, the interfacial fracture toughness of the model interface is determined using a standard four point bending (FPB) technique from samples made in at least two separate wafer fabrication processes. In this technique, the interfacial fracture toughness ($G_c$) can be determined from eq 1.

$$G_c = \frac{21(1-\nu^2)P_c^2L^2}{16Eb^2h^3} \tag{1}$$

Where $\nu$ and $E$ represent Poisson's ratio and Young's modulus of the Si substrate. In addition to mechanical properties, geometric parameters of the test sample in eq 1 are the distance between the inner and outer pins ($L$), width of the beam ($b$), and thickness of the half height of beam ($h$). A depiction of the test sample is shown in Figure 3. The critical force ($P_c$) is measured during the experiment and used to calculated $G_c$. The value of $G_c$ calculated from eq 1 represents the steady state
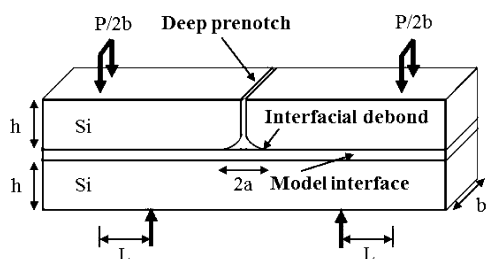
**Figure 3.** Deep prenotched FPB specimen with geometric parameters.

interfacial fracture toughness subjected to a constant moment condition, when the interface crack length (a) is very long compared to the substrate thickness.[32] As a result, $G_c$ becomes independent of film stack and interface crack length.[17] In this work, the loading rate is fixed at 0.5 μm/sec and the phase angle ($\psi$) is 43°. All tests were carried out at room temperature conditions.

Following the FPB tests it was necessary to accurately determine the exact failure location among the many layers present in our test sample. Hence, X-ray photoelectron spectroscopy (XPS) using a Thermo K-Alpha X-ray photoelectron spectroscope with an Al 1486 X-ray source was used to scan the two fracture surfaces to determine the elemental composition of the fracture surfaces. To examine the surface morphology after the FPB tests, we conducted atomic force microscopy (AFM, Veeco) in tapping mode using a NSC15 cantilever (Micromasch USA) with an average tip radius of 10 nm. Additional details are discussed in the result section.

**2.3. Contact Angle Measurements.** Polar and dispersive surface energies of the SiN$_x$ and PMMA substrates were determined through contact angle measurements using liquids (with known surface energies and characteristics) to evaluate the permanent and instantaneous dipole−dipole reactions at the SiN$_x$ and PMMA interface. Contact angles using DI water as the polar liquid and diiodomethane as the nonpolar liquid were measured on surfaces, and were converted to surface energies using a harmonic mean method (eq 2),[33] where $\gamma$ represents the surface tension, subscripts 1 and 2 refer to different liquids that were used in this work, p and d represent the polar and dispersive components, and s indicates the specific surface. This method has been used previously to measure the polar and dispersive surface energies of surfaces such as ITO, Ni200 alloy, polymer films (polymethyl metacrylate (PMMA), polycarbonate (PC), and polypropylene (PP), etc.).[21,33,34,35]

$$(1 + \cos\theta_1)\gamma_1 \quad 4\left(\frac{\gamma_1^d \gamma_s^d}{\gamma_1^d + \gamma_s^d} + \frac{\gamma_1^p \gamma_s^p}{\gamma_1^p + \gamma_s^p}\right)$$

$$(1 + \cos\theta_2)\gamma_2 \quad 4\left(\frac{\gamma_2^d \gamma_s^d}{\gamma_2^d + \gamma_s^d} + \frac{\gamma_2^p \gamma_s^p}{\gamma_2^p + \gamma_s^p}\right) \quad (2)$$

**2.4. Interface Modification Process.** Various methods to improve the interfacial adhesion strength through plasma treatments and molecular interface modifiers were explored. Traditionally, organosilanes have been used to promote adhesion by creating chemical or physical interactions at interfaces between inorganic and organic materials.[19,23] However, organosilanes tend to form multilayers or yield nonuniform surface coverage due to homocondensation.[36] Therefore, more recently, phosphonic acids (PAs) have shown

promise as another adhesion promoters by forming strong covalent bonds with metal oxides in addition to providing more robust and stable bonds compared to organosilanes.[23,37,38]

As discussed above, to vary the surface energy at the interface, we investigated three different treatments of the SiN$_x$ surface. First, oxygen (O$_2$) plasma activation (Yes R1 Plasma Cleaner: 6 min, O$_2$: 1.5 slm, and 700 W) and a thin layer of Al$_2$O$_3$ capping were used to increase the polar component of the surface energy on SiN$_x$. Second, phosphonic acids (PAs) with different tail groups to vary surface energies were used. Phosphonic acid modification of the substrates consisted of activating and cleaning the surface with O$_2$ plasma. For this purpose, a Surfx Atomflo TM 300 Series plasma tool was used at an atmospheric pressure for 10 min at 140 W. This treatment was performed to remove carbonaceous contamination, and also introduce hydroxyl groups that enabled the PA headgroup to covalently bond with the substrate.[18,21] Immediately after plasma treatment, the surfaces were immersed in a 10 mM solution of PA in ethanol for 1 h at 75 °C. After the immersion, we rinsed the substrates with ethanol followed by sonication in a solution of 5% (v/v) triethylamine in ethanol to remove any physisorbed PA molecules from the substrates, leaving covalently bound PA molecules on the surface. In this study, two types of PAs were used; 4-methoxycarbonylbutyl phosphonic acid (MCBPA) and octadecyl phosphonic acid (ODPA) as shown in Figure 4b, c. MCBPA and ODPA were purchased from Epsilon Chimie and Sigma-Aldrich, respectively.
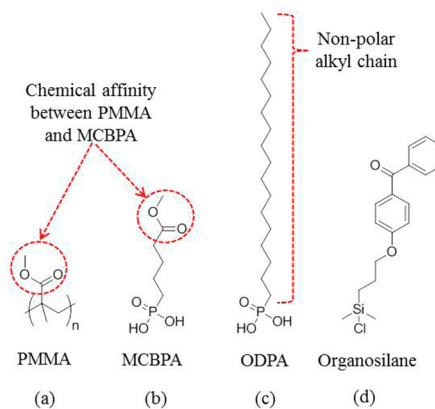


**Figure 4.** Structures of PMMA, phosphonic acid modifiers, and silane-based modifier used in this study: (a) PMMA, (b) MCBPA (4-methoxycarbonylbutyl phosphonic acid), (c) ODPA (octadecyl phosphonic acid), and (d) benzophenone derivative (4-(3′-chlorodimethylsilyl) propyloxybenzophenone silane).

Lastly, SiN$_x$ utilized benzophenone derivatized organosilanes, which have been discussed to form strong covalent bonds at the model interface,[24−26] were used in this study. In particular, a monochlorosilane (4-(3′-chlorodimethylsilyl)-propyloxybenzophenone silane), as shown in Figure 4d, was chosen in order to avoid the homocondensation reactions previously mentioned. This silane was synthesized in a manner similar to that reported in the literature,[22] and used instead of benzophenone containing phosphonic acid because PAs will not covalently bind with bare SiN$_x$ as explained in 3.2.2. In the case of the silane, the SiN$_x$ surface was treated for 3 min with oxygen plasma followed by immediate immersion in a toluene solution containing the benozophenone silane (15 mM) under a flow of nitrogen. Several drops of anhydrous triethylamine

6714

dx.doi.org/10.1021/am301880y | ACS Appl. Mater. Interfaces 2012, 4, 6711−6719

**Table 1. Summary of Experimental Sample Structures, Interfacial Fracture Toughness (J/m$^2$), and Surface Energy (mJ/m$^2$), where "IM" Indicates Interface Modification with O$_2$ Plasma and Phosphonic Acid (PA) Treatments$^a$**

| structure | interface modification (IM) | total surface energy ($\gamma^p$) (mJ/m$^2$) | dispersive component ($\gamma^p$) (mJ/m$^2$) | polar component ($\gamma^p$) (mJ/m$^2$) | $G_c$(J/m$^2$) |
|---|---|---|---|---|---|
| SiN$_x$-PMMA | × | 59.68 ± 0.71 | 32.12 | 27.56 | 4.58 ± 0.85 |
| SiN$_x$-IM-PMMA | O$_2$ plasma treatment | 72.93 ± 0.37 | 29.74 | 42.20 | 9.44 ± 1.15 |
| SiN$_x$-Al$_2$O$_3$−PMMA | × | 71.39 ± 1.85 | 31.88 | 39.51 | 7.72 ± 0.62 |
| SiN$_x$-Al$_2$O$_3$−IM-PMMA | O$_2$ plasma treatment | | | | 10.03 ± 0.94 |
| SiN$_x$-Al$_2$O$_3$−IM-PMMA | MCBPA | 56.96 ± 0.68 | 32.37 | 24.59 | 7.78 ± 0.73 |
| SiN$_x$-Al$_2$O$_3$−IM-PMMA | ODPA | 33.30 ± 0.10 | 29.76 | 3.54 | 0.84 ± 0.27 |

$^a$Surface energies of O$_2$ plasma activated SiN$_x$/Al$_2$O$_3$ surfaces are not shown because reliable contact angle measurements were difficult to obtain because of the large polar component that led to a superhydrophilic surface.

(0.5 mL) were added in an effort to promote the binding based on previous reports in the literature[39] and the substrate was allowed to remain in solution overnight. Following overnight modification, the surface was rinsed with chloroform and dried under a flow of nitrogen. In order to initiate the photochemical reactions between bezophenone derivatives and PMMA, 400 nm of PMMA was spin-cast on the silane soaked SiN$_x$ surface followed by UV exposure (Stratagene UV Stratalinker 2400, 60 min, 300 nm irradiation and a Rayonet RPR-100 photoreactor, 45 min, 350 ± 50 nm) in a similar manner to what has been reported previously.[22,23]

## 3. RESULTS AND DISCUSSION

### 3.1. Interfacial Fracture ToughnesS OF SiN$_x$−PMMA Interfaces.
To determine the baseline value of the interfacial fracture toughness of the model SiN$_x$−PMMA interface, we prepared and tested three separate sample batches amounting to a total of 39 samples. The initial results summarized in Table 1 show that the interfacial fracture toughness ($G_c$) of the SiN$_x$−PMMA interface was 4.58 ± 0.85 J/m$^2$. Figure 5a shows a
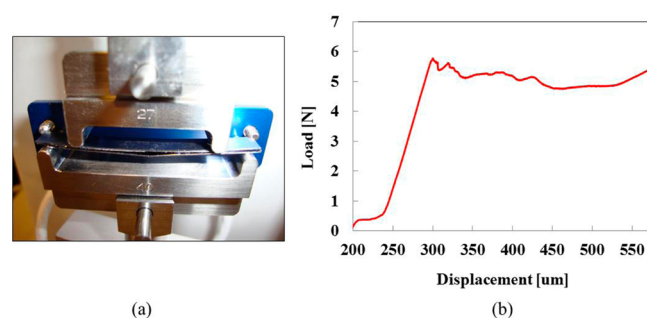


**Figure 5.** (a) Delaminated sample during FPB tests and (b) a typical load vs displacement curve obtained in this study.

delaminated sample during FPB tests and Figure 5b describes a typical load vs displacement response that was measured in this study. To determine the exact location of delamination, we used X-ray photoelectron spectroscopy (XPS) to identify the elemental composition of the delaminated surfaces. Figure 6a depicts the delaminated sample after FPB tests, and Figure 6b, c show the XPS scans for the inorganic side (SiN$_x$, 100 nm) and the organic side (PMMA, 400 nm). As shown in Figure 6b, c, there is distinct evidence of a N1s peak (~398.08 eV) on the inorganic side, while there is no N1s peak on the organic side. The XPS data therefore indicates that the delamination took place at the desired interface between SiN$_x$ and PMMA, thus

supporting the idea that the measured $G_c$ value (4.58 ± 0.85 J/m$^2$) corresponds to the interfacial fracture toughness of the model interface (SiN$_x$−PMMA).

### 3.2. Adhesion Promotion at Model Interface through Surface Energy Treatment. *3.2.1. O$_2$ Plasma Treatment.*
To explore the effect of the permanent dipole−dipole interactions on changing interfacial adhesion, we used an oxygen plasma treatment system (Yes R1 Plasma Cleaner: 6 min, O$_2$: 1.5 slm, and 700 W) to treat the SiN$_x$ surface prior to depositing the PMMA. As previously mentioned, O$_2$ plasma activation is expected to introduce polar hydroxyl groups onto the surfaces. Contact angle measurements were made on multiple samples between 10 and 15 min after oxygen plasma treatment. This is consistent with the waiting time used before depositing the PMMA on SiN$_x$ when making the SiN$_x$/PMMA barrier films and thus represents the surface energy the interface sees during barrier fabrication. Contact angle measurements performed on all substrates in this study are shown in Table 1 where the polar and dispersive energy components are calculated and compared. O$_2$ plasma-treated SiN$_x$ showed a 13.25 mJ/m$^2$ increase in its surface energy compared to bare SiN$_x$ with a higher polar component of 42.20 mJ/m$^2$ when compared to 27.56 mJ/m$^2$ for bare SiN$_x$. Four point bending tests conducted on O$_2$ plasma activated SiN$_x$ bonded to PMMA showed increased adhesion strength of 9.44 ± 1.15 J/m$^2$ compared to untreated SiN$_x$ (4.58 ± 0.85 J/m$^2$). The increase in $G_c$ value supports our hypothesis that an increase in the polar component of the surface energy on a substrate leads to increased permanent dipole−dipole interactions between the substrate and the PMMA. These dipole−dipole interactions are generally stronger than the instantaneous dipole−dipole interactions induced by the dispersive component of the surface energy,[20,40] thus enhancing the adhesion at the interface.

Although O$_2$ plasma activation of substrates improves adhesion, it is a time sensitive process where the effects of the plasma activation will diminish over time if the bonding is not performed immediately after activation. Therefore, a more permanent method of increasing the surface polarity was explored through the deposition of a thin layer of Al$_2$O$_3$ deposited by atomic layer deposition (ALD) on top of the SiN$_x$. From the literature, it is well-known that the increase of the thickness of Al$_2$O$_3$ also increases the number of surface hydroxyl groups.[41] An extremely thick layer, however, is not desirable because the increased time scale of the deposition. Therefore, 10 nm of Al$_2$O$_3$ was deposited on top of the SiN$_x$ surface to create more permanent interactions from its high
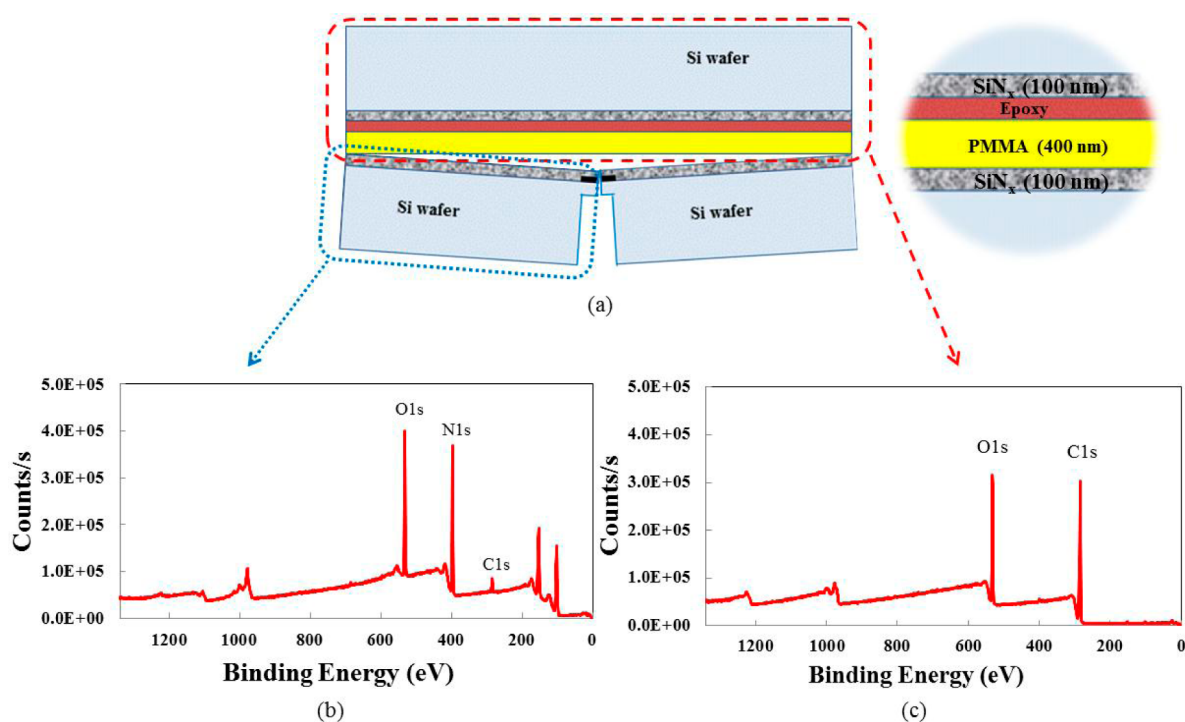
**Figure 6.** (a) Schematic diagram of the FPB sample after the delamination tests, (b) XPS scan for inorganic side containing $SiN_x$ film, and (b) XPS scan for organic side containing PMMA film.
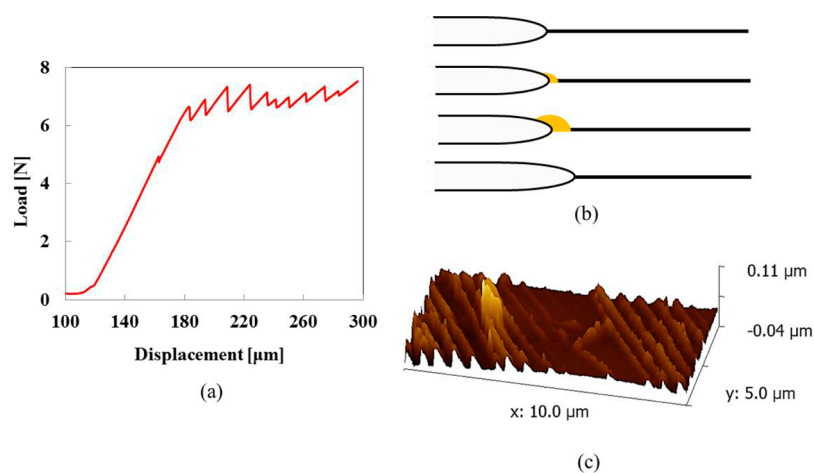


**Figure 7.** (a) Load vs displacement curve of $SiN_x/Al_2O_3$−PMMA interface, (b) crack propagation mechanism of $SiN_x/Al_2O_3$−PMMA interface where the plastic zone is extending during FPB tests until it reach the limiting point and the crack tip progresses forward, and (c) a three-dimensional (3D) atomic force microscopy (AFM) scan of $SiN_x/Al_2O_3$−PMMA interface after the FPB test.

polarity. An added advantage of depositing the $Al_2O_3$ layer is that it serves as a capping layer to the barrier and is expected to enhance its barrier performance by filling micro defects that exist in the $SiN_x$ film, leading to a lower water vapor transmission rate.[42] Contact angle measurements were performed on the $Al_2O_3$ layer and showed an increase of 11.95 mJ/m$^2$ in the polar component of the surface energy over bare $SiN_x$. Four point bending tests of the $SiN_x/Al_2O_3$−PMMA interface showed that the interfacial fracture toughness ($G_c$) increased to 7.72 ± 0.62 J/m$^2$ with the addition of the 10 nm of $Al_2O_3$ capping layer. XPS scans of the delaminated surfaces also determined that delamination occurred at the $Al_2O_3$ and PMMA interface demonstrating the effect of increased polarity on the interface bond strength. While the increase in $G_c$ by

addition of the 10 nm thick $Al_2O_3$ capping layer was not as high as that of $O_2$ plasma treated $SiN_x$, it is still higher than a bare $SiN_x$−PMMA interface, whereas also providing enhanced barrier performance as discussed earlier. The effect of further enhancing the polarity of the $Al_2O_3$ capped $SiN_x$ on the interfacial adhesion strength was explored by $O_2$ plasma treatment of the $Al_2O_3$ layer. Contact angle measurements in the case of $O_2$ plasma activated $SiN_x/Al_2O_3$ surfaces were difficult because of the large polar component that led to a superhydrophilic surface. FPB tests conducted on $O_2$ plasma activated $SiN_x/Al_2O_3$ bonded to PMMA showed increased adhesion strength 10.03 ± 0.94 J/m$^2$ compared to 7.72 ± 0.62 (J/m$^2$) obtained for untreated $SiN_x/Al_2O_3$−PMMA interface

and similar to that of $O_2$ plasma-activated uncapped $SiN_x$–PMMA interface ($9.44 \pm 1.15$ J/m$^2$).

Interfacial surface energy modification through increased polarity also produced changes in the crack tip behavior at the model interface when compared to the unmodified interface. The load vs displacement data for $SiN_x$/$Al_2O_3$–PMMA interface is shown in Figure 7a. This periodic hardening and softening in the load vs displacement response originated from an energy dissipation effect at the crack tip during the FPB tests. When the crack propagates along the $SiN_x$/$Al_2O_3$–PMMA interface, it extends its plastic zone size by dissipating the energy at the crack tip until it reaches a limiting point where the PMMA film cannot maintain its integrity any longer, as described in Figure 7b. Beyond this critical point, the crack tip quickly breaks through the plastic zone, and progresses forward, as observed through atomic force microscope (AFM) scans of the delaminated region ($Al_2O_3$ side after FPB tests) in Figure 7c. This hardening and softening pattern of the crack propagation as observed from the load vs displacement curve is also observed in the surface morphology of the $Al_2O_3$ deposited $SiN_x$ surface after the FPB tests.

*3.2.2. Phosphonic Acid Modifications.* To conduct surface modification of $SiN_x$ using PAs, it was hypothesized that the previously discussed $Al_2O_3$ capped $SiN_x$ would be required since PAs are typically used in the modification of metal oxides.[18] To confirm the inability of PAs to modify $SiN_x$, we used pentafluorobenzyl phosphonic acid (PFBPA) as an initial test surface modifier. This particular molecule was chosen due to the large number of fluorine atoms present on the tail benzyl group. If the modification, would prove to be successful, an intense F1s peak would be observed in the XPS spectrum, as previously reported.[21] In this study, it was found that XPS analysis of $SiN_x$ surfaces after attempted PA modification (according to literature methods for metal oxides[21]) lacked the presence of any fluorine confirming the inability of PAs to directly modify $SiN_x$. Therefore, in order to study the effect of PA surface modification on the interface adhesion, it was decided to conduct all investigations using the $Al_2O_3$-capped $SiN_x$. Before modifying the model interface using the PAs, the ability of the PFBPA to covalently bond to the $Al_2O_3$ capping layer was verified through dip coating and subsequent XPS analysis, wherein the F1s peak from PFBPA was clearly observed.

Surface energy modification using PAs can be performed by varying the polarity of the tail group where a benzyl, fluorine or methyl terminating tail group commonly result in low polar energy component, whereas amines or hydroxyl tail groups commonly result in increased polarity.[18] Although phosphonic acids bind to the $Al_2O_3$-capped $SiN_x$ through covalent bonds,[43] the headgroup of the PAs is expected to bind to the PMMA through weak secondary bonds such as van der Waals forces. These two features of molecular interface modifiers as in the case of phosphonic acids provide us with two distinctive modes to modify the interfacial fracture strength; (a) by varying the polarity of the surface through suitable choice of the PA tail group and (b) through the chemical affinity effect between the PMMA and the PA by matching the PA tail group to the PMMA.

For this purpose, two different PAs (MCBPA and ODPA) were identified based on the surface energy of the tail groups after modification, as shown in Figure 4. MCBPA (Figure 4b) has the same tail group (methoxy group; O–CH$_3$ and carbonyl group; O=C) as PMMA and is therefore expected to produce

a strong interface because of its chemical affinity with PMMA (shown in Figure 4a, b). As expected, even though the polarity of the MCBPA modified $SiN_x$/$Al_2O_3$ surface (24.59 mJ/m$^2$) was similar to that of bare $SiN_x$ surface (27.56 mJ/m$^2$), the interfacial fracture toughness increased almost by a factor of 2 (4.58–7.78 mJ/m$^2$) because of the chemical affinity between the PMMA and MCBPA that potentially enabled them to form a strong interface. However, the improvement in adhesion through enhanced compatibilization of $SiN_x$/$Al_2O_3$ and PMMA using MCBPA (7.78 mJ/m$^2$) was still lower than that measured with $O_2$ plasma activated $Al_2O_3$/$SiN_x$–PMMA interface (10.03 mJ/m$^2$) indicating that the polar component of the surface energy at the interface dominates the interfacial adhesion by inducing more permanent dipole interactions rather than the tail group matched interface that results in a weaker bond.

The second PA modifier, ODPA (Figure 4c) was chosen because of its low polarity (3.54 mJ/m$^2$). As expected, the ODPA modified surface weakened the interfacial fracture toughness, and was measured to be 0.84 mJ/m$^2$. The weak bond may have resulted from the large number of instantaneous dipole–dipole interactions induced between the highly nonpolar ODPA and the PMMA dominating the interface strength and minimizing any contribution from the polar component of the surface energy.

*3.2.3. Benzophenone Modification.* Results from FPB tests for the benzophenone silane treatment of the SiNx–PMMA interface show that the interfacial fracture toughness increased by a factor of 5 compared to that of the unmodified SiNx–PMMA interface (27.78 $\pm$ 2.83 and 4.58 $\pm$ 0.85 J/m$^2$, respectively). This enhancement in the interfacial fracture toughness is likely due to the strong covalent bonds between the benzophenone tail group attached to the organosilane and PMMA through photochemical reactions initiated by irradiation with UV light.[22,29] Among the three chemical surface modification methods explored in this study, the benzophenone silane treatment produced the largest enhancement in interfacial fracture strength for a constant PMMA thickness of 400 nm.

As discussed in section 3.2.2, the choice of organosilane treatment of the interface was driven by the fact that PAs will not covalently bond to a bare $SiN_x$ surface. However, on the basis of the current results, the modification time required for a PA versus a chlorosilane is much shorter (a few minutes for PAs vs 24 h modification for silanes) and PA modification shows better long-term shelf stability compared to organosilanes,[23,37,38] which make them more attractive for barrier applications. Moreover, the use of the $Al_2O_3$ capping layer to enable the PA modification of the $SiN_x$ surface will also lead to lower water vapor transmission rate (g/m$^2$/day),[42] as discussed in section 3.2.1. Although surface treatment utilizing the benzophenone silane provided the largest $G_c$ value, the more complicated methodology compared with that of $O_2$ plasma-activated $SiN_x$/$Al_2O_3$–PMMA makes it less appealing, particularly after considering that $O_2$ plasma treated interface on its own produces adhesion strength as high as 10.03 $\pm$ 0.94 J/m$^2$. Thus, further research is needed on rapid deposition of benzophenone derived interface modifiers in order to enable their integration in barrier film manufacturing.

**3.3. Adhesion Promotion through Mechanical Modification of the Model InterfaceA.** Previous research with poly(arylene) ether (PAE), showed that a plastic zone size is constrained by two stiff elastic layers in a sandwich structure that strongly influences the interfacial fracture toughness.[44] In

our model, SiN$_x$–PMMA structure, the plastic zone size is also constrained by the thickness of the PMMA layer that is sandwiched between the stiff Si substrates as shown in Figure.1. To further investigate the effect of energy dissipation at the crack tip as a function of plastic zone size, three different SiN$_x$–PMMA interfaces with 120 nm, 400 nm, and 2.16 $\mu$m of PMMA layers were fabricated, and tested using four point bending (FPB) tests. The results are summarized in Table 2,

**Table 2. Summary of Three Different PMMA Thicknesses (120 nm, 400 nm, and 2.16 $\mu$m) in the Basic SiN$_x$–PMMA Model Interface with Corresponding Interfacial Fracture Toughness Values**

| thickness of PMMA | interfacial fracture toughness (J/m$^2$) |
| --- | --- |
| 120 nm | 1.47 ± 0.43 |
| 400 nm | 4.58 ± 0.86 |
| 2.16 $\mu$m | 13.12 ± 0.66 |

and showed that the interfacial fracture toughness of the SiN$_x$–PMMA interface was enhanced from 1.47 ± 0.43 J/m$^2$ in the case of the 120 nm thick PMMA to 13.12 ± 0.66 J/m$^2$ in the case of the 2.16 $\mu$m of PMMA. Althiugh the theoretical plastic zone size of the PMMA layer is approximately 33 $\mu$m, and is significantly thicker than our entire FPB structure, the interfacial fracture strength is enhanced by almost three times compared to our model structure just by reducing the constraint on the plastic zone at the crack tip obtained by increasing the thickness of the PMMA layer.

## 4. CONCLUSIONS

The various factors affecting interfacial fracture toughness of a model SiN$_x$–PMMA interface were studied and quantified using a four point bending technique. The effect of surface energy modification at the interface was studied through the introduction of polar capping layers and O$_2$ plasma activation where the adhesion strength of the SiN$_x$–PMMA interface was almost doubled from 4.58 J/m$^2$ (SiN$_x$–PMMA) to 10.03 J/m$^2$ (SiN$_x$/Al$_2$O$_3$–PMMA) through increased surface polarity. Phosphonic acids with various tail groups were also used to chemically treat the interface to have both chemical affinity as well as to further investigate the importance of surface polarity at the interface. Although the chemical affinity of the two contact materials at the interface enhanced the adhesion strength to 7.78 mJ/m$^2$, we conclude that the polar energy of the surface energy dominantly affects interfacial fracture toughness by enabling strong permanent dipole–dipole interactions as observed by the large improvement in adhesion obtained in the case of O$_2$ plasma treated substrates (10.03 mJ/m$^2$). The use of benzophenone, which has been shown to produce strong covalent bonds with polymer overlayers,[22] at the model interface resulted in a five times enhancement of adhesion strength. However, even though this type of surface treatment maximized the adhesion strength, it would not be the ideal candidate for barrier applications because of its more complex and lengthy processing conditions. Additionally, interfacial adhesion was also increased through mechanical modification of the structure where the plastic zone size at the crack tip was varied by changing the thickness of the PMMA layer and found to increase the fracture toughness by three times. Overall, our study shows that increasing the polarity of the interface through surface treatments and increasing the plastic zone size are effective in enhancing the interfacial

adhesion strength and reliability of hybrid organic–inorganic barrier layers while ensuring the integrity of the barrier.

## AUTHOR INFORMATION

**Corresponding Author**
*E-mail: sgraham@gatech.edu.

**Notes**
The authors declare no competing financial interest.

## REFERENCES

(1) Meyer, J.; Gorrn, P.; Bertram, F.; Hamwi, S.; Winkler, T.; Johannes, H. H.; Weimann, T.; Hinze, P.; Riedl, T.; Kowalsky, W. *Adv. Mater.* **2009**, *21*, 1845.
(2) Dameron, A. A.; Davidson, S. D.; Burton, B. B.; Carcia, P. F.; McLean, R. S.; George, S. M. *J Phys Chem C* **2008**, *112*, 4573.
(3) Choi, J. H.; Kim, Y. M.; Park, Y. W.; Park, T. H.; Jeong, J. W.; Choi, H. J.; Song, E. H.; Lee, J. W.; Kim, C. H.; Ju, B. K. *Nanotechnology* **2010**, *21*, 1361.
(4) Choi, D.-w.; Kim, S.-J.; Lee, J. H.; Chung, K.-B.; Park, J.-S. *Curr. Appl. Phys.* **2012**, *12*, s19.
(5) Chiang, C. C.; Wuu, D. S.; Lin, H. B.; Chen, Y. P.; Chen, T. N.; Lin, Y. C.; Wu, C. C.; Chen, W. C.; Jaw, T. H.; Horng, R. H. *Surf. Coat. Technol.* **2006**, *200*, 5843.
(6) Singh, B.; Bouchet, J.; Rochat, G.; Leterrier, Y.; Manson, J. A. E.; Fayet, P. *Surf. Coat. Technol.* **2007**, *201*, 7107.
(7) Graff, G. L.; Williford, R. E.; Burrows, P. E. *J. Appl. Phys.* **2004**, *96*, 1840.
(8) Han, Y. C.; Jang, C.; Kim, K. J.; Choi, K. C.; Jung, K.; Bae, B. S. *Org. Electron.* **2011**, *12*, 609.
(9) Kim, N. *Ph.D. Dissertation.* Georgia Institute of Technology, Atlanta, GA, 2009; pp55
(10) Andersons, J.; Modniks, J.; Leterrier, Y.; Tornare, G.; Dumont, P.; Manson, J. A. E. *Theor. Appl. Fract. Mech.* **2008**, *49*, 151.
(11) Leterrier, Y. *Prog. Mater. Sci.* **2003**, *48*, 1.
(12) Leterrier, Y.; Andersons, J.; Pitton, Y.; Manson, J. A. E. *J. Polym. Sci. Polym. Phys.* **1997**, *35*, 1463.
(13) Lewis, J. *Mater. Today* **2006**, *9*, 38.
(14) Lewis, J.; Grego, S.; Vick, E.; Chalamala, B.; Temple, D. *Mater. Res. Soc. Symp. Proc.* **2004**, *814*, 189.
(15) Leterrier, Y.; Waller, J.; Manson, J. A. E.; Nairn, J. A. *Mech. Mater.* **2010**, *42*, 326.
(16) Kook, S. Y.; Dauskardt, R. H. *J. Appl. Phys.* **2002**, *91*, 1293.
(17) Dauskardt, R.; Lane, M.; Ma, Q.; Krishna, N. *Eng. Fract. Mech.* **1998**, *61*, 141.
(18) Hotchkiss, P. J.; Jones, S. C.; Paniagua, S. A.; Sharma, A.; Kippelen, B.; Armstrong, N. R.; Marder, S. R. *Acc. Chem. Res.* **2012**, *45*, 337.
(19) Jenkins Borrego, M.; H. D., R.; Bravman, J. C. *J. Microelectron. Electron. Packag.* **2007**, *5*, 8.
(20) Wu, S. *Polymer Interface and Adhesion*; Marcel Dekker: New York, 1982.
(21) Paniagua, S. A.; Hotchkiss, P. J.; Jones, S. C.; Marder, S. R.; Mudalige, A.; Marrikar, F. S.; Pemberton, J. E.; Armstrong, N. R. *J. Phys. Chem. C* **2008**, *112*, 7809.
(22) Prucker, O.; Naumann, C. A.; Ruhe, J.; Knoll, W.; Frank, C. W. *J. Am. Chem. Soc.* **1999**, *121*, 8766.
(23) Ohashi, K. L.; Yerby, S. A.; Dauskardt, R. H. *J. Biomed. Mater. Res.* **2001**, *54*, 419.
(24) Yanez, J. A.; Baretzky, B.; Wagner, M.; Sigmund, W. M. *J Eur Ceram Soc* **1998**, *18*, 1493.

6718

dx.doi.org/10.1021/am301880y | ACS Appl. Mater. Interfaces 2012, 4, 6711–6719

(25) Cahill, B. P.; Giannitsis, A. T.; Land, R.; Gastrock, G.; Pliquett, U.; Frense, D.; Min, M.; Beckmann, D. *Sens. Actuator, B* **2010**, *144*, 380.

(26) Hohlfelder, R. J.; Maidenberg, D. A.; Dauskardt, R. H.; Wei, Y. G.; Hutchinson, J. W. *J. Mater. Res.* **2001**, *16*, 243.

(27) Swanson, M. J.; Opperman, G. W. *J. Adhes. Sci. Technol.* **1995**, *9*, 385.

(28) Czech, Z. *Polym. Bull.* **2004**, *52*, 283.

(29) Park, H. S.; Gong, M. S. *Macromol. Res.* **2010**, *18*, 596.

(30) Chang, B. J.; Prucker, O.; Groh, E.; Wallrath, A.; Dahm, M.; Ruhe, J. *Colloid Surf., A* **2002**, *198*, 519.

(31) Lane, M. *Annu. Rev. Mater. Res.* **2003**, *33*, 29.

(32) Charalambides, P. G.; Lund, J.; Evans, A. G.; McMeeking, R. M. *J. Appl. Mech., Trans. ASME* **1989**, *56*, 77.

(33) Kim, J. S.; Friend, R. H.; Cacialli, F. *J. Appl. Phys.* **1999**, *86*, 2774.

(34) Chan-Park, M. B.; Gao, J. X.; Koo, A. H. L. *J. Adhes. Sci. Technol.* **2003**, *17*, 1979.

(35) Kitova, S.; Minchev, M.; Danev, G. *J. Optoelectron. Adv. Mater.* **2005**, *7*, 249.

(36) Mutin, P. H.; Guerrero, G.; Vioux, A. *CR Chim.* **2003**, *6*, 1153.

(37) Mutin, P. H.; Guerrero, G.; Vioux, A. *J. Mater. Chem.* **2005**, *15*, 3761.

(38) Sharma, A.; Kippelen, B.; Hotchkiss, P. J.; Marder, S. R. *Appl. Phys. Lett.* **2008**, *93*, 163308-1.

(39) Tripp, C. P.; Hair, M. L. *J. Phys. Chem.* **1993**, *97*, 5693.

(40) EgeS. N. *Organic Chemistry: Structure and Reactivity*; Houghton Mifflin: Boston, 2004.

(41) Wind, R. A.; George, S. M. *J. Phys. Chem. A* **2010**, *114*, 1281.

(42) Kim, N.; Potscavage, W. J.; Domercq, B.; Kippelen, B.; Graham, S. *Appl. Phys. Lett.* **2009**, *94*, 163308-1.

(43) Thissen, P.; Valtiner, M.; Grundmeier, G. *Langmuir* **2010**, *26*, 156.

(44) Brand, V.; Bruner, C.; Dauskardt, R. H. *Sol. Energy Mater. Sol. Cells* **2012**, *99*, 182.